Design Report 2

Alex Tofini & Ana Ciocoiu
Department of Electrical and Computer Engineering,
University of British Columbia
(Dated: December 15, 2021)

In this project, a circuit containing multiple co-planar waveguide resonators operating within a range of 4-8 GHz with and without SQUID arrays is designed and laid out for fabrication. The SQUIDs are used to shift the resonance frequency of the resonator when added in series with them and the lone resonators are used as fail-safe designs. The fabricated design will be mounted on a PCB and measured with a VNA to probe the aforementioned resonant frequencies.

I. INTRODUCTION

A superconducting nanowire single-photon detector (SNSPD) is an optical and near-infrared photon detector. They offer single-photon sensitivity with high detection efficiency, low dark count rates, and fast recovery time, making them attractive for sensing and communications applications [1]. An SNSPD consists of a superconducting nanowire held below its critical temperature and biased just below its critical current. When a single photon impinges on the detector, Cooper pairs are broken and the local critical current will reduce below that of the bias current, forming a resistive hot-spot in that area. The resistance is typically larger than that of a readout amplifier, leading to the current getting shunted through this external circuit. This provides a measurable voltage signal. A typical readout circuit for SNSPDs is created by connecting each detector to a cryogenic low-noise amplifier, then amplifying the signal further at room temperature and digitizing the final output [2]. This readout scheme becomes very challenging for multi-element SNSPDs, as the increased number of coax lines causes a significant heat load to the cryostat and increased complexity. A readout scheme using a CPW resonator and SQUIDs is proposed. The signal from an SNSPD can be used to bias a SQUID, either directly through a bias tee or using a flux bias line. These two options are illustrated in Fig. 3. The resonance frequency of the circuit is given by the CPW resonator, and the SQUID acts like a variable inductor. In the case of a single-photon detection event, the current from the SNSPD will bias the SQUID, changing the resonance frequency of the circuit. By correctly designing the circuit, this resonance frequency shift should be detectable on a VNA. For this project, the SNSPD will be replaced with a simple current source, to simplify the operation and testing of the circuit. If the circuit is functioning as intended, it can be integrated to work with the SNSPDs at a later date.

II. FUNDAMENTALS

A Josephson Junction (JJ) consists of two superconducting electrodes separated by an insulating barrier. At a temperature below the critical temperature (Tc) of the metal, electron in the metal become paired and drop to a lower energy state. This opens up an energy gap, and the pair is allowed to tunnel across the junction without any resistance so long as the current is below the critical current I_c of the junction. The current fluctuates as a periodic function of the phase difference between the electrode wavefunctions, $I = I_c sin\delta$, where δ is the phase difference.

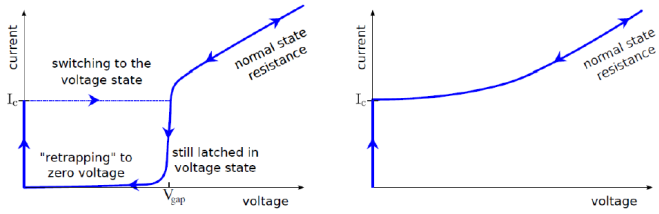

FIG. 1. From [3]. The current-voltage charactersitics of an underdamped (left) and overdamped (right) JJ are shown. A JJ can be made to operate as overdamped by appropriate choice of a shunt resistor.

A high-quality JJ will have a hysteretic I-V relationship: the voltage will jump abruptly to a non-zero value once I exceeds I_c, but will only return to zero once the current is reduced significantly below I_c. This hysteresis must be eliminated for SQUIDs to operate in a conventional manner: usually, this is accomplished through the use of a shunt resistor.

The I-V characteristics of JJs can be explained by the resistively- and capacitively-shunted junction (RCSJ) model. The Stewart-McCumber parameter β_c arises as a result of this model, and is written as:

$$\beta_c = \frac{2\pi}{\Phi_0} I_c R^2 C, \tag{1}$$

where R is the shunt resistor, C the junction capacitance, and Φ_0 the flux quantum. In the strongly overdamped limit, $\beta_c \ll 1$.

A SQUID is composed of two parallel JJs within a superconducting loop. The superconducting ring can be biased with a current I, and placed in a magnetic field that applies a flux Φ to the loop. The JJs will limit the maximum current that can flow within the loop to the sum of each junction's critical current $I_c = I_{c1} + I_{c2}$. The

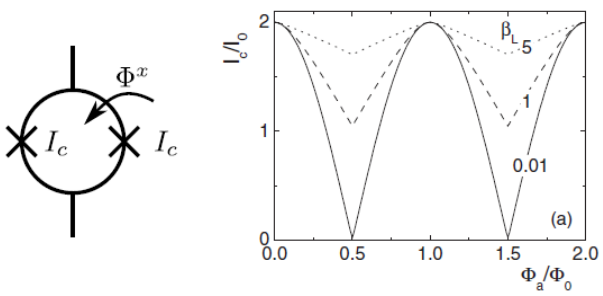

FIG. 2. Left: A circuit depiction of a SQUID. Right: Assuming non-negligible self-inductance, the current-flux characteristics of a SQUID are plotted for different values of β_L.

magnetic flux enclosed inside the superconducting loop will modulate the critical current of the SQUID with a period of Φ_0. This behavior can be exploited in a variety of ways: a common use of the SQUID is as a flux-to-voltage converter. However, in this case, the SQUID will be used as a tunable inductor.

Assuming negligible self-inductance, the critical current of the SQUID is [4]:

$$I_c = 2I_o \mid cos(\pi \frac{\Phi}{\Phi_0}) \mid, \tag{2}$$

where Φ is the applied flux and I_0 the critical current of the JJ. For the case of a realistic design, the modulation depth of this current-flux relationship is determined by the screening parameter $\beta_L = 2LI_0/\Phi_0$, where L is the inductance of the SQUID washer. For the best modulation depth, $\beta_L \ll 1$ [5].

An expression for SQUID inductance that includes the effect of the washer inductance is found in [4] and written as:

$$L_j(\Phi, i) = L_{jo}(\Phi) + Ai^2 = \frac{\phi_0}{I_c(\Phi)}(1 + \beta_L \frac{cos2f}{2cosf}) + \frac{\phi_0}{2{I_c}^3} i^2, \tag{3}$$

Where $\phi_0 = \frac{\Phi_0}{2\pi}$, $f = \pi \frac{\Phi}{\Phi_0}$, and i is the biasing current.

A CPW resonator with central conductor width w and spacing s is quite simple to design with the use of a few equations [6]. The characteristic impedance of the resonator is given as

$$Z_0 = \sqrt{\frac{\mu_0}{16\epsilon_0\epsilon_{eff}}} \frac{K(k_0')}{K(k_0)} \tag{4}$$

where K are elliptic integrals and $k_0 = \frac{w}{w+2s}$, $k_0' = \sqrt{1-{k_0}^2}$.

The inductance and capacitance per unit length are also found using elliptic integrals:

$$L' = \frac{\mu_0}{4} \frac{K(k_0')}{K(k_0)} \tag{5}$$

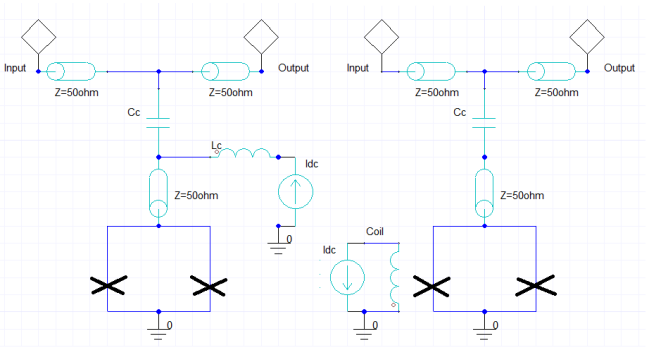

FIG. 3. Left: Biasing with a DC current source using a bias tee inductor L_c.Right:Inductive biasing with a flux loop. The value of L_c is chosen to not interfere with the centre frequency of the resonator.

$$C' = 4\epsilon_0\epsilon_{eff} \frac{K(k_0)}{K(k_0')} \tag{6}$$

The total length of the CPW is selected as a fraction of the wavelength at the resonance frequency, in this case, $\lambda/4$.

By putting a SQUID in series with this resonator, the total inductance of the circuit can be increased when the SQUID is biased, shifting the resonance frequency. Since the inductance of the SQUID depends on both the applied flux Φ and the biasing current i, the inductance of the SQUID can be changed through either a direct DC current bias line or an inductive coupling coil. Both methods are shown in Fig. 3. If a greater shift in resonance frequency is needed to be detectable, several SQUIDs can be arrayed in series.

III. DESIGN

A. Calculations

The design procedure for a resonator with a centre frequency of 5.5 GHz is shown here. First, the value of k_0 can be found from a plot of (4). For a 50 Ω impedance, the value of k_0 should be 0.564. If a width $w = 5\mu m$ is selected for the CPW, then the spacing will be $s = 1.93\mu m$. For an ϵ_{eff} of 5.22 for Si, the length of a $\lambda/4$ resonator is found to be 5.9673 mm.

The inductance and capacitance per unit length are found to be $L' = 3.809\text{e-}07\ H/m$ and $C' = 1.524\text{e-}10\ F/m$. From the analytic S_{21} parameter graph in Fig. 4, it is possible to approximate the coupling quality factor Q_c of the resonator. A coupling capacitor value of $C_c = 10fF$ is used, and the quality factor is therefore $Q_c \approx 5200$, according to the expression $Q_c = f_c/FWHM$.

The total quality factor can be found by taking into account the loss tangent of the dielectric. For silicon,

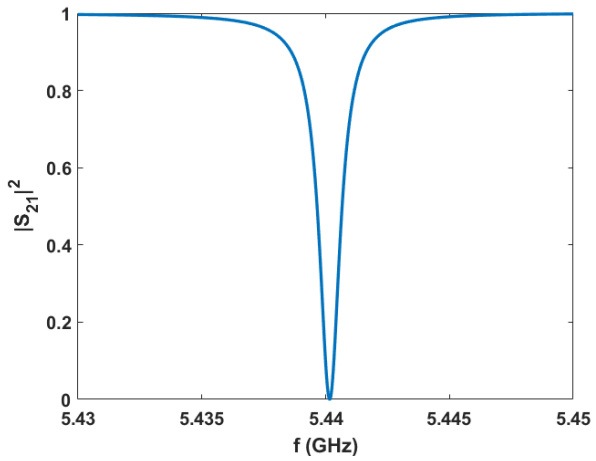

FIG. 4. Plot of transmission as a function of frequency showing a slightly shifted resonance frequency at 5.44GHz. The FWHM is approximated 1.018 MHz, due to the coupling capacitor value of 10 fF. The curve is computed using equations for admittance in Pozar [7].

$\delta \approx 0.01$ at 5.5 GHz. Since $Q^{-1} = {Q_c}^{-1} + tan\delta$, $Q \approx$ 2700.
However, this might be quite simplistic, since the loss tangent depends strongly on doping and temperature. Doping information is not available, so it is difficult to determine what effect 4K temperatures will have on the Q factor of the design.

Resonators with centre frequencies of 4.5, 6.5, and 7.5 GHz were also designed.

For the case of a DC current bias, the inductance of the SQUID washer is of little importance: an existing layout design was simulated in ANSYS HFSS and the inductance was determined to be 68 pH.This design is shown in Fig. 12. The geometry of the washer, including the size of the hole and length of the gap affect this inductance value [8]. It was found that our simulation result aligns closely with the expression for total inductance from literature [8].

Five different options for JJ area, and therefore, critical current were given to us for the StarCryo process [9]. The critical current density J_c is 100 A/cm^2, and the AuPd sheet resistivity is 1.3 Ω/sq. Since it is necessary to design for $\beta_c \ll 1$, the value of the shunt resistor needed to achieve this must be determined. The capacitances provided to us are the junction specific capacitance $C_s = \frac{1}{22-0.75ln(Jc)}$, parasitic capacitance $C_{jp} = 4.5e^{-4}pF/\mu m^2$, and resistor capacitance $Cr = 2.25e^{-4}pF/\mu m^2$.

In the design, the overlap between the Nb2 and Tri layers is 575.84 μm^2. The area of the shunt resistor is chosen, initially, as 53.9 μm^2. The total junction capacitance arising from this calculation, along with the R_{shunt} value required for a certain β_c, is summarized in Fig. 5.

If shunt resistor dimensions are chosen to be 7 by 7.7 μm, the total resistance of 2 Ω will satisfy the design requirement for β_c for all possible junction areas.

Junction Critical Current (μA)	Total Capacitance (pF)	Bc = 0.001 $R_{shunt}(\Omega)$	Bc = 0.01 $R_{shunt}(\Omega)$
6.4	0.0109	2.1707	6.8642
8.4	0.0110	1.8862	5.9648
14.7	0.0111	1.4170	4.4810
32.2	0.0113	0.9531	3.0139
67.9	0.0113	0.6550	2.0713

FIG. 5. Table of required shunt resistance value to achieve a given β_c, as a function of different junction areas.

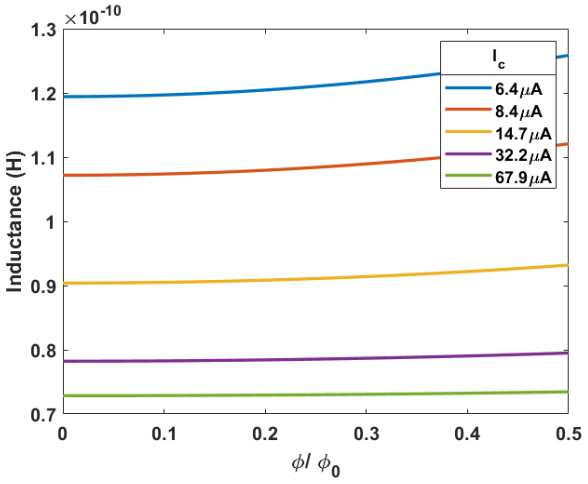

FIG. 6. Plot of inductance shift as a function of applied flux for different junction critical currents.

Next, the flux-inductance characteristics from (3) are plotted for the given critical currents in Fig. 6. The largest shift in SQUID inductance is found to occur for the smallest junction area. Therefore, the 6.4 μm^2 junction is chosen for this design.

The total shift in inductance that a single SQUID accomplishes can be found as $\delta_f = \frac{1}{2\pi\sqrt{C(L+L_{max})}} - \frac{1}{2\pi\sqrt{C(L+L_{min})}}$, where C is the total capacitance of the resonator ($9e^{-13}F$), L is the total inductance of the resonator ($2.2e^{-09}H$), and $L_{max(min)}$ is the maximum (minimum) inductance obtained from the current-biased SQUID. It is found that the shift in inductance from a single SQUID is 4.7 MHz. Therefore, creating a 5-SQUID array should produce a shift greater than 20 MHz, which should be detectable even in the case of a lower Q factor from the resonator.

Finally, a value for the bias tee inductance (from Fig. 3) L_c needs to be found. The total admittance of the circuit containing the inductor, resonator, and capacitor can be found, and the S_{21} parameters plotted. By choosing any value of inductor below 1 nH, the centre frequency of the resonator will remain largely unaffected. This is shown in Fig. 7.

The SQUID in the case of an flux bias using a loop is slightly more complicated to design, since the inductance is directly modulated by the applied flux Φ. As can be

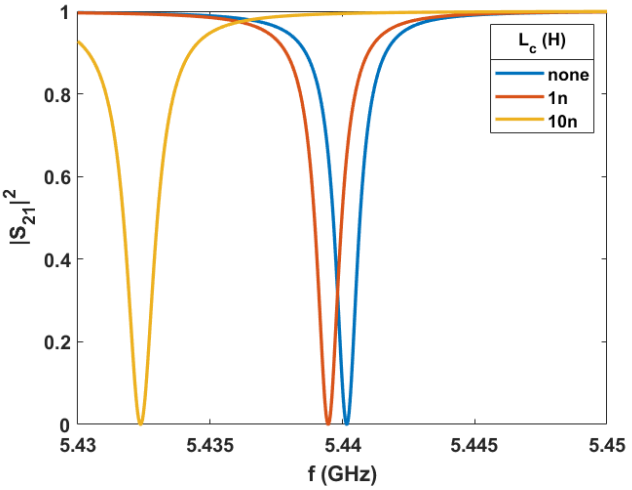

FIG. 7. Plot of transmission as a function of frequency for different L_c values. Note that the resonance frequency is not affected much if the value is smaller than 1nH.

seen from Fig. 2, the modulation depth will be reduced by half if $\beta_L \approx 1$, and will continue to decrease as β_L increases. Therefore, a SQUID must be designed to have a very small washer inductance. After several iterations, a new design was created that has a simulated inductance of 17pH, giving a β_L of 0.336. While this is not as small as we would have liked, we hope it will be sufficient. This SQUID layout design can be seen in Fig. 13.

With the non-linear term in (3) set to zero, the resulting SQUID inductance for the case of a flux bias is calculated. Based on equations from [4], the expected shift in resonant frequency due to applied flux of the resonator-SQUID array is calculated:

$$\omega_o(\Phi) = \omega_r \frac{1}{1 + N\epsilon(\Phi)}, \tag{7}$$

where ω_r is the resonant frequency of the CPW resonator, $1\sqrt{LC}$, N is the number of SQUIDs in series, and $\epsilon(\Phi)$ is given as:

$$\epsilon(\Phi) = L_{j0}(\Phi)/L \tag{8}$$

A plot of expected ω_r function of applied flux for the β_L value of 0.336 under varying N is shown in Fig 8a, and for a single SQUID under different values of β_L in Fig. 8b.

It is likely that the 17pH inductance of the SQUID design for this case is small enough to approximate the ideal case of negligible self-inductance. From Fig. 8a it also becomes apparent that a single SQUID is sufficient to detect a resonance shift.

As a final design verification step, the mutual inductance of the bias coil and 17 pH SQUID design was determined through an ANSYS two-port network simulation. Ideally, the mutual inductance should be in the nH range if we want to use small $\approx 1\mu A$ currents to bias the SQUID. The 17pH SQUID design, along with a flux-biasing coil, was simulated in ANSYS. The simulation layout is shown in Fig. 9. The mutual inductance of this design was found to be about 1pH, meaning that, if the simulation is reliable, currents in the mA range will likely be required to bias it. While not ideal, this should be feasible. The expected current output from an SNSPD is in the $\approx 10\mu A$ range, so they may be too low to be used reliably with this circuit.

B. Layout

The proposed design described here was created using StarCryo's three Nb layer process. The design consists of two AC feed lines fabricated on the ground plane that are capacitively coupled to a multitude of structures. Interdigitated capacitors were used in order to tune the capacitance to our desired values instead of using parallel plate capacitors since the coupled structures always start with co-planar waveguides (CPWs) which are located on the ground layer, seen in Fig. 10.

Prior to designing the length of the CPW resonators, the waveguide configuration had to be chosen. This was done through analytical expressions provided to us [6]. The geometry is shown in Fig. 11. With this configuration chosen, the length of each resonator was chosen such that in a $\lambda/4$ configuration it would create a unique resonance frequency to prevent signal interference between independent test structures.

The test structures we decided to investigate were a set of resonators of increasing complexity. The baseline fall back experiment consists of a single CPW meander capacitively coupled to the feed line. This simple structure was repeated for multiple different interdigitated capacitors with varying orders of magnitude for their capacitance ranging from 1 fF to 100 fF. This sweep will ideally create at least one configuration that we can successfully measure. Our more ambitious designs consist of an array of DC SQUIDS in series with CPWs. One set of these SQUIDs will be directly current biased, while another set will be flux biased. Both of these designs will be used to investigate whether a frequency shift can be detected once a current similar to that of the SNSPDs is applied. Due to the complications of simulating flux biasing in the design phase, the flux-biased case has the lowest likely success rate.

The SQUIDs utilized in our design are composed of two parallel Josephson junctions which create a path between the second Nb and the ground layer. The junctions have shunt resistors in parallel to them that span a gap on the second Nb layer and are subsequently connected and meet up with the junction paths on the ground layer. The two resulting ground layer paths are connected together through a washer-like structure thus forming a loop. The geometric properties of this loop determine the geometric inductance for the SQUID. For the flux biasing version,

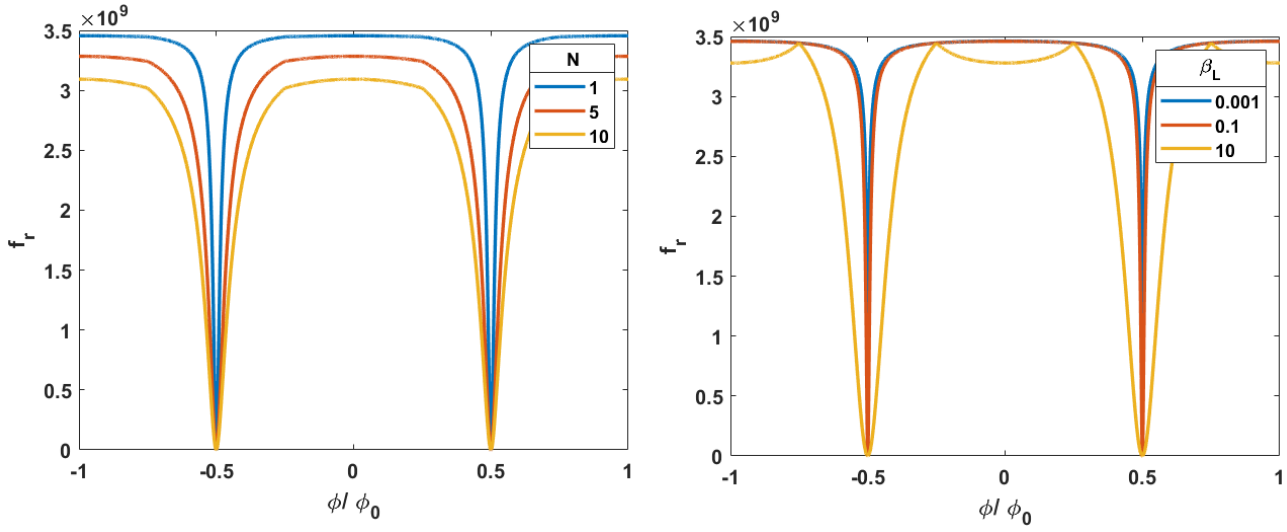

FIG. 8. A plot of expected resonance frequency shift as a function of applied flux for series combination of CPW resonator and SQUIDs. Left: constant β_L of 0.336 and varying numbers of SQUIDs. Right: A single SQUID under varying β_L values.

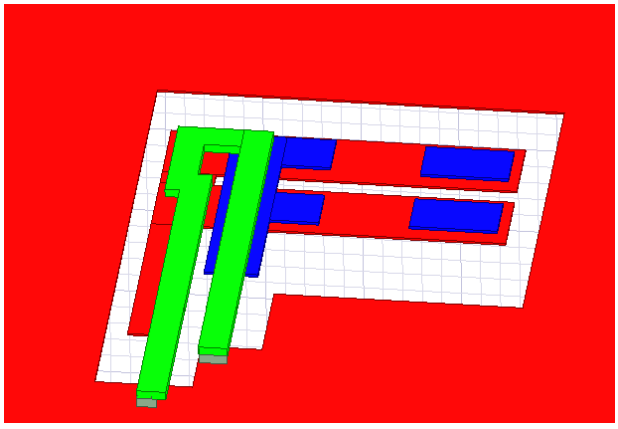

FIG. 9. 17pH SQUID design set up as a two-port network simulation in ANSYS HFSS. The flux biasing coil is light green. The SQUID washer is shown in red, lying in a cutout section of the design ground plane. The Nb2 layer is shown in blue. Resistors have been removed from the design. JJ vias not visible.

there is a spiraling loop overlaid on top of the washer located on the second Nb layer. The loop is connected to the third Nb layer through vias at the center and edge of the loop. An example for both biasing configurations is shown in Fig. 12.

The geometric inductance of the washer configuration in Fig. 12 was simulated, yielding inductance values in the $\approx 200pH$ range. It became apparent that the resulting β_L value would be much larger than 1, and therefore too large to flux bias it and obtain an appropriate modulation depth. With this taken into consideration, smaller SQUIDs (shown in Fig. 13) were designed and simulated, and found to have a much smaller inductance of $17pH$. Both designs will be fabricated in order to confirm our

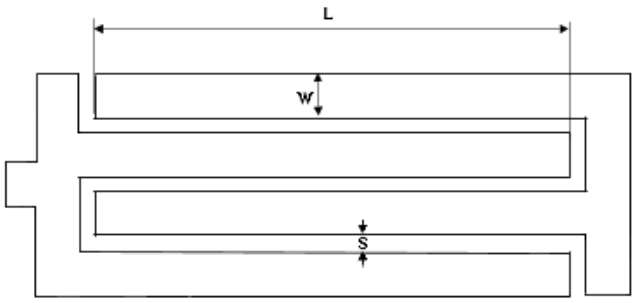

FIG. 10. In order to comply with StarCryo process restriction, the width of each finger, w, in the capacitor was set to 5 um and the separation between fingers, s, was set to 2 um. The number of fingers and the length of each finger, L, varied depending on the desired capacitance

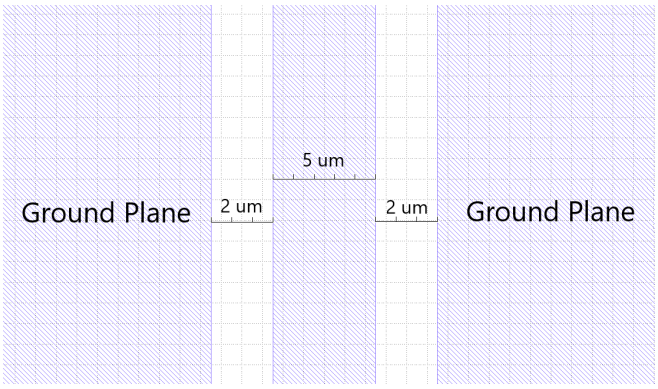

FIG. 11. The ideal design for the CPW consisted of an internal signal line of width 5 um and a 1.93 um separation to the ground plane. However due to minimum feature spacing with StarCryo this was increased to 2 um.

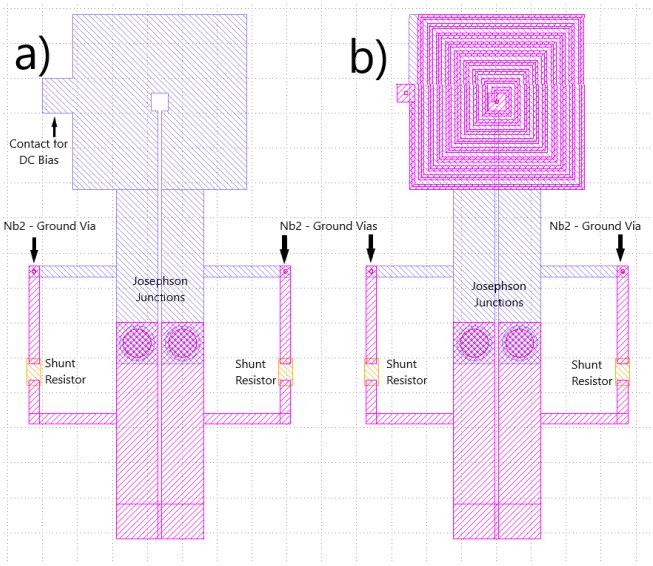

FIG. 12. a) Direct DC bias configuration without the need for a spiral on top of the washer. b) Flux biased configuration with spiral located on top of the washer.

theory regarding said geometric inductance and modulation depth.

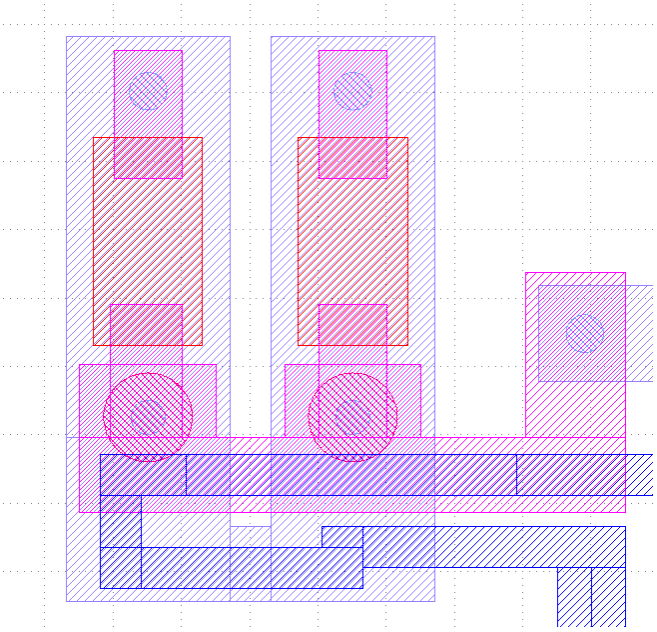

FIG. 13. By minimizing the hole in the SQUID loop, the geometric inductance was minimized. StarCryo's design rules regarding edge clearance and minimum feature size were the limiting factors on this design. The downside of the small loop size is a reduced space for the flux biasing loop above it, most likely leading to a smaller mutual inductance value.

The original proposed design was created prior to knowing the restrictions imposed by the PCB, Fig. 14, which resulted in the layout being centered around a single centered feedline which was incompatible with the PCB. The final design proposed here in Fig. 15 addresses this issue with two independent feedlines, one for the resonators with SQUIDs and one for stand-alone resonators. In addition to modifying the feedlines, the new design contains reworked bond pads which have been relocated to be compatible with the PCB. Lastly the bond pads' gold contact layer was removed to allow for direct bonding to the Nb layer as requested by StarCryo.

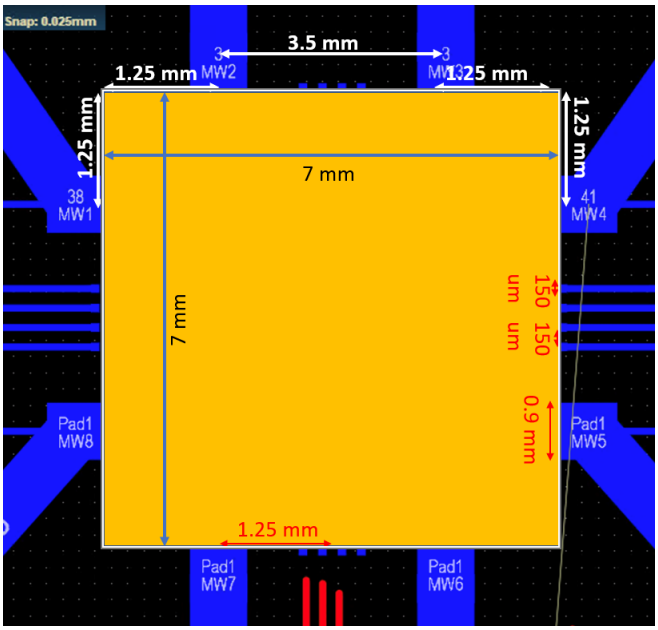

FIG. 14. This provided PCB configuration allows for 8 microwave feed lines and 16 DC lines. Measurement typo persists in this version.

C. Design Limitations

This section describes the fundamental limitations to the designed devices due to the fabrication restrictions imposed by StarCryo, such as minimum feature size, minimum spacing and minimum overlap. The first design proposed in Report 1 was formulated based off the original DRC rules provided by StarCryo. However, upon submission, we were informed that there were additional rules that needed to be followed. These new rules resulted in the need for significant changes to the design, mainly for the miniature SQUID as shown in Fig. 16. There were two DRC rules that were not made clear during the original design phase: the shunt resistor layer must be enclosed by the TRI layer at all times, and the via exclusion on the JJ prevents the minimum junction area reported by StarCryo from being achievable. The JJ had to be significantly increased in size in order to comply with this DRC rule. These changes resulted in a cascading series of DRC violations since the original design was optimized to match the DRC rules exactly; any size

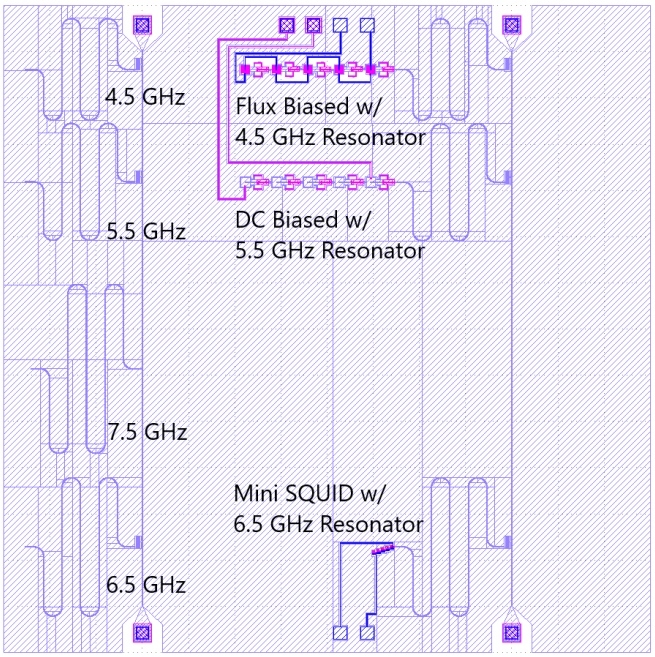

FIG. 15. Annotated layout depicting independent CPWs that form the first phase of testing, as well as the flux biased and DC current biased SQUID arrays in series with CPW resonators of varying centre frequencies.

increase to a given part in the SQUID required modifications to all other parts. After multiple iterations, a new optimized SQUID was created which is about 10% larger than the original design, and thus will have an increased geometric inductance. The next significant layout error involved polygons with too many points, i.e 2000+ points. This error occurred due to our use of a ground plane that covered the entire chip, something that is required for superconducting chips. This DRC rule was not included in the original explanation therefore was not considered until this second design iteration. Since the GDS file was created using KLayout, the polygons are handled slightly differently and required some editing to be compatible with L-Edit. This editing consisted of merging every single object in the TRI layer together and slicing them into sections with less than 2000 points which can be automatically done by saving the file in a compressed format.

On top of the abundance of real DRC errors present in the original design there existed an immense amount of false DRC errors present in the design as a result of polygon discretization, which were ignored. These types of errors occur when a designer pushes the process to the limit and creates an object with the exact minimum feature size, the exact spacing, the exact overlap, etc. In the case of Manhattan structures, no complications arise from this. However, when curvature is introduced the discretization results in edges that violate the rules. Typically these types of errors are avoided altogether by including a tolerance in the DRC checker, but it appears that StarCryo's PDK does not contain said feature.

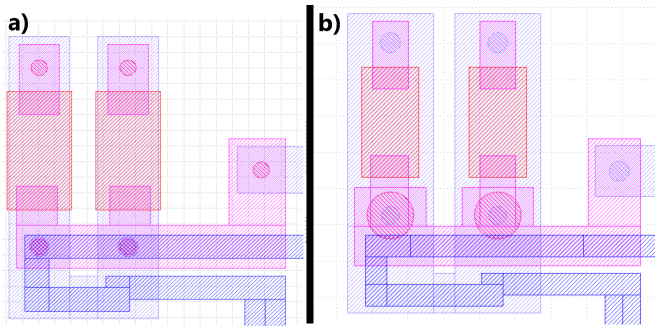

FIG. 16. a) Original miniature SQUID design that required modifications. b) Modified miniature SQUID design that now complies with the new DRC rules.

D. Measurement Plan

Once fabricated, the chip will be glued to the 7x7 mm chip slot located on the PCB and wirebonding will be used to connect the DC lines and microwave lines to their corresponding pads on chip. The chip will be mounted in a cryostat at 4K. Since the microwave feed lines are connected to co-axial cable mounts on the PCB, we will be able to use a vector network analyzer (VNA) and probe all the capacitively coupled designs on each line and determined the s-parameters. First, the individual CPW resonators will be probed to determine whether their resonance frequency lies within the expected range. Since each resonator was designed to operate within a range of 4-8 GHz as mentioned above, the VNA available to us (operates up to 12GHz) should be adequate to detect the response of each design. The VNA and cryo setups are available at QFL in Sherbrooke, but we may attempt to create this circuit at UBC using existing equipment.

Next, the steady-state response of the SQUID array will be investigated. This will be done by directly biasing the SQUIDs using a current source connected via the bias tee, or by connecting the current source to the flux biasing loop of the SQUID. In both cases, the current source should be able to ouptut at currents in the $mA - \mu A$ range. We will sweep the current to create different flux biasing conditions, and probe the response with a VNA. Ideally, we should be able to detect a resonance frequency shift in real-time, similar to the graph in Fig. 7. This readout scheme, adapted from [10], is illustrated in Fig. 17.

If the first test is successful, we will attempt to simulate the behavior of SNSPDs by using an AC current source to bias the SQUIDs. The source should have pulse amplitudes in the μA range, with nanosecond duration. Responses of this speed should still be visible on the VNA.

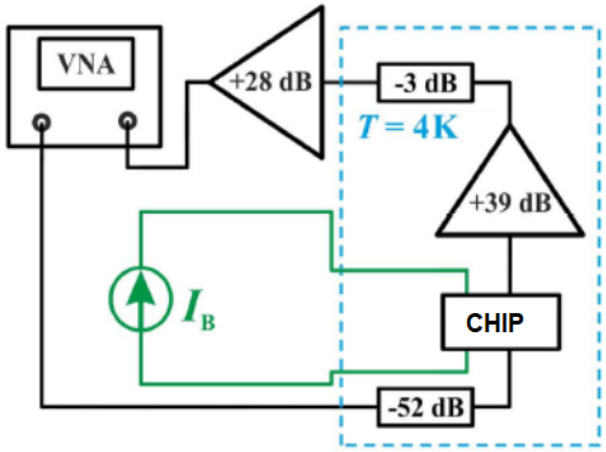

FIG. 17. Measurement circuit adapted from [10]. I_b denotes the current source used for biasing. The transmitted microwave signal can be amplified using a 39 dB cryogenic broadband high-electron mobility transistor low-noise amplifier (HEMTLNA). Ideally, thermal noise from the VNA probe will be attenuated with a -52dB cold attenuator.

IV. CONCLUSION

We aim to create the first iteration of a circuit that will eventually be used to read out SNSPDs. Since we are unable to include real SNSPD's in our testing stages, we will simply bias a series of DC SQUIDs in an attempt to change their inductance, and thus affect the resonance frequency of the circuit (which is given by a CPW). The current design aims to investigate whether these SQUID arrays are capable of sufficiently manipulating the resonance frequency of the CPWs. In the event that we are unable to flux bias the SQUIDS we created a fail-safe direct DC biased version, which is less sensitive to the geometric inductance of the SQUID. In the event that the larger SQUIDS are unsuccessful, we have included a miniature SQUID that has the smallest geometric inductance based off the restrictions of the StarCryo design rules.

V. ACKNOWLEDGEMENT

The authors would like to give a big thank you to Mark Volkmann from D-Wave for his continuous technical support. Also would like to thank Joe Salfi and Rogerio de Sousa for their support and feedback after the workshop. We also thank QSciTech and QuantumBC for organizing this workshop.

REFERENCES

[1] M. K. Akhlaghi, E. Schelew, and J. F. Young, Waveguide integrated superconducting single-photon detectors implemented as near-perfect absorbers of coherent radiation, Nature **6** (2015).
[2] T. Ortlepp, M. Hofherr, L. Fritzsch, S. Engert, K. Ilin, D. Rall, H. Toepfer, H.-G. Meyer, and M. Siegel, Demonstration of digital readout circuit for superconducting nanowire single photon detector, Optics express **19** (2011).
[3] M. Volkmann, Activity 4.1: Squids, qpfs, and sfq circuits, Superconducting Workshop **1** (2021).
[4] A. Palacios-Laloy *et al.*, Tunable resonators for quantum circuits, Journal of low temperature physics **151** (2008).
[5] J. Clarke and A. I. Braginski, Squid design, in *The SQUID Handbook* (Wiley, Darmstadt, 2006) Chap. 2.
[6] J. Salfi, Activity 2.2: Cpw resonator tutorial, Superconducting Workshop **1** (2021).
[7] D. M. Pozar and P. (Firm), *Microwave engineering* (Wiley, 2012).
[8] Q. Zhang *et al.*, EnglishGeometric dependence of washer inductance for nbn dc squids, IEEE transactions on applied superconductivity **28**, 1 (2018).
[9] R. Cantor, Ten-level low-tc josephson junction process specifications, StarCryo Fab Documentation **1** (2021).
[10] S. Doerner, A. Kuzmin, K. Graf, I. Charaev, S. Wuensch, and M. Siegel, Compact microwave kinetic inductance nanowire galvanometer for cryogenic detectors at 4.2 k, Journal of Physics Communications **2** (2018).